Highly C2/C1-Selective Covalent Organic Frameworks Substituted with Azo Groups

Shaofeng Huang, Yiming Hu, Li-Li Tan, Shun Wan,* Sadegh Yazdi, Yinghua Jin,* and Wei Zhang*

ABSTRACT: A series of covalent organic frameworks substituted with azo groups (AzoCOFs) have been synthesized via imine condensation. The obtained frameworks show crystallinity and high stability. More importantly, the AzoCOFs exhibit exceptionally high ideal adsorption solution theory (IAST) selectivity in adsorption of C_2H_2 (35−2891) over CH_4 at 273 K and 1 bar, owing to the favorable interactions between azo groups and acetylene molecules. The dependence of the gas adsorption property on pore size and polarity of the frameworks was also studied. The triethylene glycol substituted **Tg-AzoCOF** shows the highest C_2H_2/CH_4 selectivity (IAST selectivity of 2891), which represents the highest reported for all porous materials. The AzoCOFs also exhibit high IAST adsorption selectivity of C_2H_4/CH_4 (11−20), C_2H_6/CH_4 (15−22), and CO_2/CH_4 (12−37), which is comparable with most porous materials, thus showing their great potential in gas separation applications.

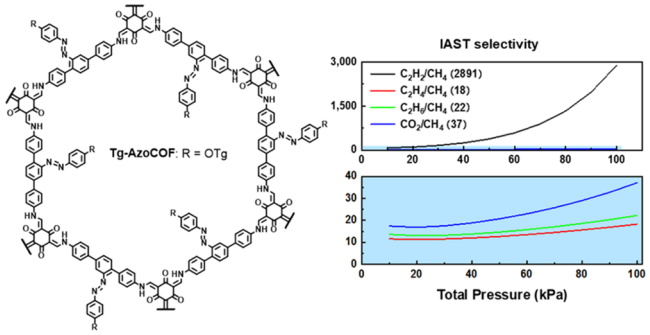

KEYWORDS: *covalent organic framework, azo group, imine condensation, selective gas adsorption, C_2/C_1 separation*

1. INTRODUCTION

C2 hydrocarbons, including acetylene, ethylene, and ethane, are important raw materials in the industry.[1] The separation of C2 hydrocarbons from methane has been a key industrial process, which can upgrade the quality of natural gas and provide an alternative source of C2. However, the conventional cryogenic distillation, which separates the C2/C1 molecules by their different boiling points or vapor pressure, is very energy consuming. In recent years, the gas separation using microporous adsorbents has been extensively explored as an alternative efficient and cost-effective approach. Among porous polymeric materials, covalent organic frameworks (COFs)[2] have been developed as novel absorbents with a tremendous potential in various gas separation and storage applications within the past decade.[3−5] COFs are crystalline, pure organic porous materials with low density.[6] The covalent bonds make the framework structure stable under most common conditions. Moreover, COF structures can be predesigned through the principles of reticular chemistry and dynamic covalent chemistry,[7] rendering the great tunability of the size and function of inside pores.[8−11] In general, COFs can be prepared under conventional solvothermal conditions, which makes COFs easy to be scaled-up and good candidates as adsorbent materials for an industrial process. However, so far, only a handful of pure organic polymers have been reported for C2/C1 separation. MCOF-1 is the first reported COF used in size-selective C2/C1 separation. It has a 3D framework structure with boronic ester linkages, which are sensitive to moisture.[12] Recently, a series of Hexene-CTF polymers with triazine linkage[13] have also been used for C2/C1 separation, where the separation mechanism is the $\pi-\pi$ interaction between the unsaturated C2 molecule and the triazine core as well as the unsaturated aliphatic linker.

The azo group is a well-known functional group with high polarity and repulsion interaction with nonpolar molecules.[14] It can act as a Lewis base center and strongly interact with acidic molecules. Many porous polymers containing azo groups in their backbones have been reported for gas separation.[15−17] However, the mobility of such azo groups when located in the backbone is rather restricted and their interaction with guest molecules is limited. To the best of our knowledge, although acetylene has high acidity (~10^{20} higher than saturated hydrocarbons) and could have strong interactions with azo groups, COFs with azo groups have not been investigated for selective adsorption of acetylenes. Herein, we designed a series of imine-linked COF structures with azo groups installed as side chains inside the pores. Three different AzoCOFs, either unsubstituted, or substituted with nonpolar alkyl chains or polar triethylene glycol chains have been synthesized to tune

the size and polarities of the pores and study the structure−property relationship. All three AzoCOFs show excellent adsorption selectivity of C2 unsaturated hydrocarbons (particularly acetylene) and carbon dioxide over methane due to their favorable interactions with azo groups. Among them, **Tg-AzoCOF** with polar triethylene glycol (Tg) chains exhibits an unprecedentedly high IAST selectivity of 2891 (1 bar) and Henry's law selectivity of 26 toward acetylene adsorption over methane at 273 K.

2. EXPERIMENTAL SECTION

2.1. Synthesis of Tg-AzoCOF. An ampule was charged with diamine **1-Tg** (15.8 mg, 0.03 mmol), trialdehyde **2** (4.2 mg, 0.02 mmol), *n*-butanol (0.25 mL), and an aqueous solution of acetic acid (6 M, 0.05 mL). The ampule was frozen at 77 K in liquid nitrogen and evacuated to the internal pressure of ~100 mTorr. Then, the ampule was sealed with flame and heated at 150 °C for 3 days without any stirring and disturbance. The orange powder was collected by vacuum filtration; washed with THF, CH_2Cl_2, and acetone under Soxhlet extraction for 24 h for each solvent; and dried under reduced pressure. **Tg-AzoCOF** was obtained as an orange powder (17 mg, 92%). Anal. Calcd for **Tg-AzoCOF** $(C_{37}H_{34}O_6N_4)_n$: C, 70.46; H, 5.43; N, 8.88. Found: C, 67.31; H, 5.09; N, 8.42.

2.2. Synthesis of H-AzoCOF. The same procedure described for the synthesis of **Tg-AzoCOF** was followed. **H-AzoCOF** (10 mg, 72%) was obtained as an orange powder using **1-H** (10.8 mg, 0.03 mmol), trialdehyde **2** (4.2 mg, 0.02 mmol), *n*-butanol (0.25 mL), and acetic acid (6 M, 0.05 mL). The physical data of **H-AzoCOF** is as follows: Anal. Calcd for $(C_{15}H_{10}ON_2)_n$: C, 76.91; H, 4.3; N, 11.96. Found: C, 67.84; H, 3.81; N, 6.84.

2.3. Synthesis of C_{10}-AzoCOF. The same procedure described for the synthesis of **Tg-AzoCOF** was followed. **C_{10}-AzoCOF** (15 mg, 79%) was obtained as an orange powder using **1-C_{10}** (16 mg, 0.03 mmol), trialdehyde **2** (4.2 mg, 0.02 mmol), *n*-butanol (0.25 mL), and acetic acid (6 M, 0.05 mL). The physical data of **C_{10}-AzoCOF** is as follows: Anal. Calcd for $(C_{37}H_{34}O_6N_4)_n$: C, 76.9; H, 6.45; N, 8.97. Found: C, 75.66; H, 6.34; N, 8.84.

2.4. Ideal Adsorption Solution Theory (IAST) Selectivity Calculation. All the isotherms were fitted by the dual-site Langmuir−Freundlich equation shown below.

$$n = \frac{q_1 b_1 p^{1/n_1}}{1 + b_1 p^{1/n_1}} + \frac{q_2 b_2 p^{1/n_2}}{1 + b_1 p^{1/n_2}} \tag{1}$$

where n is the amount absorbed (mmol/g), q is the saturation loading for site 1 and 2 (mmol/g), b is the Langmuir parameter associated with site 1 or 2 (kPa^{-1}), n_1 and n_2 are the factors for the adsorption associated with the site 1 or 2, and p is the pressure (kPa). The IAST selectivity was calculated by the equations shown below.

$$\pi(p) = \frac{RT}{A} \int_0^{py_1/x_1} n(p) d\ln p \tag{2}$$

$$x_1 + x_2 = 1 \tag{3}$$

$$y_1 + y_2 = 1 \tag{4}$$

$$\pi_1 = \pi_2 \tag{5}$$

$$s_{1,2} = \frac{x_1/y_1}{x_2/y_2} \tag{6}$$

where x_i is the molar fraction of the moiety i in the solution phase, y_i is the molar fraction of the moiety i in the gas phase, and $s_{1,2}$ is the selectivity of 1 over 2. R, T, and A are constants for the same adsorbate at constant temperature.

2.5. Method of Isosteric Heats Calculation. The two isotherms at different temperatures were fitted by the equation shown below.

$$\ln p = \ln N + \frac{1}{T}\sum_{i=0}^{i=5} a_i N^i + \sum_{i=0}^{i=2} b_i N^i \tag{7}$$

where p is the pressure (mmHg), N is the adsorption amount (mg/g), T is the temperature (K), and a_i and b_i are the virial coefficients. The isosteric heat was calculated by the equation shown below.

$$Q_{st} = -R\sum_{i=0}^{i-5} a_i N^i \tag{8}$$

where R is the universal gas constant.

3. RESULTS AND DISCUSSIONS

We synthesized three azo-containing COFs, **H-AzoCOF**, **C_{10}-AzoCOF**, and **Tg-AzoCOF**, with different substituents. In a typical procedure, a mixture of diamine **1** (**1-Tg**, **1-C_{10}**, or **1-H**) and 1,3,5-triformylphloroglucinol **2** in *n*-butanol and acetic acid was heated at 150 °C for 3 days without stirring (Figure 1a). An orange powder was formed, which was collected and

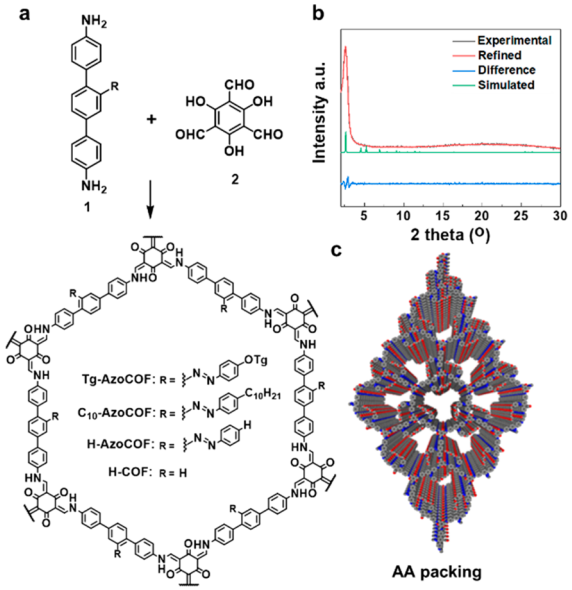

Figure 1. (a) Synthesis of AzoCOFs; (b) Experimental PXRD patterns of Tg-AzoCOF and the simulated patterns of the AA packing mode; (c) Model of Tg-AzoCOF in the AA packing mode.

washed with THF, CH_2Cl_2, and acetone via Soxhlet extraction (24 h for each solvent) to provide the product AzoCOFs (72−92%). All AzoCOFs were characterized by solid-state NMR spectroscopy, IR spectroscopy, powder X-ray diffraction (PXRD), N_2 adsorption isotherms, and thermogravimetric analysis (TGA).

The ^{13}C cross-polarization magic-angle spinning (CP-MAS) NMR spectra of all three AzoCOFs show resonance peaks around 185−195 ppm and 107−108 ppm corresponding to the carbonyl carbons and α-enamine carbons of β-ketoenamine, the peaks around 148−150 ppm corresponding to the enamine carbon (=CNH), and the peaks around 160−170 ppm corresponding to the carbons connected to the azo bonds (Figures S1−S3). For **Tg-AzoCOF**, we observed the carbon resonance peaks of triethyleneglycol chains around 55−80 ppm (Figure S1). The peaks corresponding to the decyl chain carbons in **C_{10}-AzoCOF** were observed around 68 ppm and 14−30 ppm (Figure S3). The Fourier transform infrared (FTIR) spectra of all three AzoCOFs show the disappearance

of the aldehyde peak at 1633−1634 cm^{-1} and appearance of the newly formed β-ketoenamine stretch at 1620−1621 cm^{-1} (Figure S4−S6).

The crystallinity of all AzoCOFs was proved by PXRD measurements. All AzoCOFs exhibit decent crystallinity, showing an intense peak at 2θ = 2.70° and two small peaks at 2θ = 4.70° and 5.50°, corresponding to the planes (100), (110), and (200), respectively (Figure 1b and Figures S7 and S8). Unit cell parameters of all AzoCOFs were refined by the Pawley method to be $\alpha = \beta = 90°$, $\gamma = 120°$, $a = b = 38.8$ Å, and $c = 3.5$ Å. Crystal lattice packing of all AzoCOFs were determined to be a fully eclipsed AA stacking mode with an interlayer distance of 3.5 Å (Figure 1c). The simulated PXRD patterns match well with the experimental results. The crystallinity of AzoCOFs was also confirmed by the TEM images, which clearly show layered structures with d spacing of 0.32−0.38 nm (Figures S64−S66).

Although **Tg-AzoCOF** and **C_{10}-AzoCOF** are crystalline, they are almost nonporous, showing a BET surface area of 28−29 m^2/g and a pore volume of <0.1 cm^3/g, presumably due to the long alkyl chains and Tg chains occupying the effective pores. **H-AzoCOF** without long side chains shows a considerably higher BET surface area of 245 m^2/g (Table S4) and a larger pore volume of 0.26 cm^3/g. The pore size distribution calculated using quenching solid density functional theory (QSDFT) shows pores with the diameter around 2.4 nm in **H-AzoCOF** (Figure S16). TGA analyses show all AzoCOFs are stable up to 350 °C (Figures S9−S11).

Next, N_2, CO_2, CH_4, C_2H_2, C_2H_4, and C_2H_6 are chosen as the probe molecules to examine the gas adsorption properties of AzoCOFs. All measurements were conducted at 1 bar and 273 and 295 K (Figure 2, Figures S17−S19, and Table 1). At

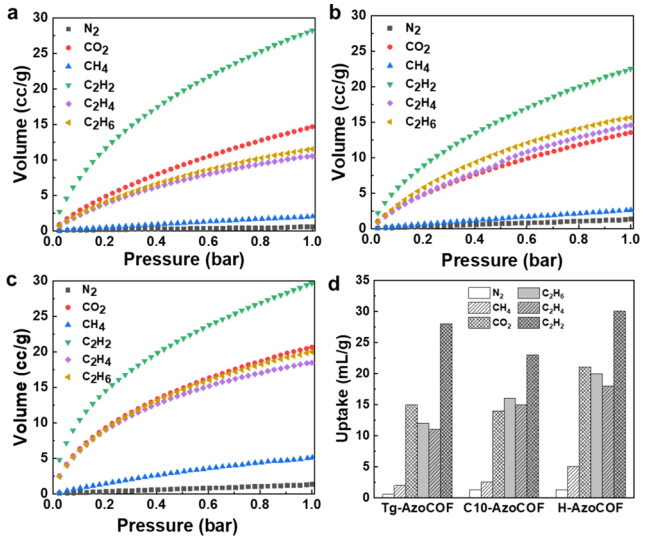

Figure 2. Gas adsorption isotherms of Tg-AzoCOF (a), C_{10}-AzoCOF (b), and H-AzoCOF (c) at 273 K and the comparison graph (d).

273 K and 1 bar, the uptakes of **Tg-AzoCOF** toward N_2, CH_4, CO_2, C_2H_6, C_2H_4, and C_2H_2 were 0.57, 2.0, 15, 12, 11, and 28 mL/g, respectively (Figure 2a). At the same temperature and pressure, the uptakes of CH_4, C_2H_4, and C_2H_6 in **C_{10}-AzoCOF** are increased around 30%, reaching 2.6, 15, and 16 mL/g, respectively (Figure 2b). However, the uptake of C_2H_2 in **C_{10}-AzoCOF** is decreased by 20% compared to the amount adsorbed in **Tg-AzoCOF** (23 vs 28 mL/g). This difference in acetylene uptake is probably due to the favorable interactions of the Lewis basic triethylene glycol chain in **Tg-AzoCOF** with more acidic acetylene molecules. **H-AzoCOF**, with a relatively higher surface area than the other two AzoCOFs, has considerably higher uptake for all gas molecules except nitrogen.

At the same temperature and pressure, the uptakes of N_2, CH_4, CO_2, C_2H_6, C_2H_4, and C_2H_2 in **H-AzoCOF** were 1.3, 5.1, 21, 20, 18, and 30 mL/g, respectively (Figure 2c). The gas uptakes in **C_{10}-AzoCOF** and **H-AzoCOF** follow the similar trend, showing the increasing uptake in the order of $N_2 < CH_4 < CO_2 \approx C_2H_6 \approx C_2H_4 < C_2H_2$. The differences in gas adsorption properties of AzoCOFs were similar at 295 K and 1 bar (Table 1).

To obtain a deeper understanding on the adsorption selectivity of AzoCOFs, we also examined Henry's law selectivity calculated based on the ratio of initial slopes (0−0.1 bar) for each pair of gas molecules (Table 2). The slope of the adsorption isotherms at a low pressure range, which is far from the saturation point, is indicative of the affinity of gas molecules to the absorbents when the diffusion rate is similar. The initial adsorption slopes of acetylene, ethylene, and CO_2 adsorption isotherms in **Tg-AzoCOF** are much higher than those observed for **C_{10}-AzoCOF**, whereas the initial slopes of the methane and ethane adsorption isotherms are higher in **C_{10}-AzoCOF** than **Tg-AzoCOF**. Since the surface areas of **Tg-AzoCOF** and **C_{10}-AzoCOF** are similar, it suggests that **Tg-AzoCOF** has a higher affinity towards unsaturated hydrocarbons and more acidic molecules, while **C_{10}-AzoCOF** has a higher affinity toward saturated hydrocarbons. **H-AzoCOF**, which has almost nine times higher surface area, shows the highest initial slopes for all the gas molecules likely due to their fast diffusion. The Henry's law selectivity of AzoCOFs was then calculated. As shown in Table 2, **Tg-AzoCOF** shows the highest Henry's law selectivity of acetylene over methane at both 273 K (26) and 295 K (22), suggesting the highest binding affinity of **Tg-AzoCOF** for acetylene is due to its most basic pore environment. The **Tg-AzoCOF** and **C_{10}-AzoCOF** have almost the same Henry's law selectivity for ethylene over methane at 273 and 295 K. **C_{10}-AzoCOF** shows the highest selectivity of ethane over methane likely because its pores have saturated hydrocarbon chains with a similar structure to ethane. **H-AzoCOF** shows the lowest selectivity of C2 and CO_2 over methane at 273 K due to its mesoporous nature, which has relatively weaker interactions with those gas molecules.

Henry's law selectivity only reflects the real mixture selectivity at a very low pressure (0−0.1 bar) and low loadings on the adsorbent materials. For practical applications, we deal with gas mixtures under saturated adsorption conditions. Thus, we used an ideal adsorption solution theory (IAST) method[23,18] to calculate the selectivity for binary gas mixtures. The IAST selectivity at 1 bar with equimolar gas mixtures are listed in Table 2. It is interesting to note that **Tg-AzoCOF** has an extremely high C_2H_2/CH_4 selectivity (2891)[19] and good selectivity for C_2H_4 (18), C_2H_6 (22) and CO_2 (37) over CH_4 at 273 K and 1 bar. Such selectivity of C_2H_2 over CH_4 is the highest among all the reported materials, including both pure organic polymers and metal organic polymers (Table 3). Although the IAST selectivity of **H-AzoCOF** toward C_2H_2 over CH_4 is much lower than that of **Tg-AzoCOF** (123 vs 2891) at 273 K, it is still among the highest reported. The

Table 1. Summary of Gas Uptake of AzoCOFs at Low Pressure[a]

	273 K[a]						295 K[a]					
samples	N_2	CO_2	CH_4	C_2H_2	C_2H_4	C_2H_6	N_2	CO_2	CH_4	C_2H_2	C_2H_4	C_2H_6
Tg-AzoCOF	0.57	15	2.0	28	11	12	0.68	7.6	1.1	17	6.4	6.6
C_{10}-AzoCOF	1.3	14	2.6	23	15	16	1.2	9.0	2.0	18	9.0	11
H-AzoCOF	1.3	21	5.1	30	18	20	1.2	14	3.9	25	14	15

[a]1 bar; unit of uptake: mL/g (volumes have already been converted to STP).

Table 2. Summary of the Ideal Adsorption Selectivity, Henry's Law Selectivity, and IAST Selectivity[a,b]

		C_2H_2/CH_4 selectivity		C_2H_4/CH_4 selectivity		C_2H_6/CH_4 selectivity		CO_2/CH_4 selectivity	
temperature	samples	Henry's law	IAST[a]	Henry's law	IAST[a]	Henry's law	IAST[a]	Henry's law	IAST[a]
273 K	**Tg-AzoCOF**	26	2891 (2426)[b]	8.5	18	9.0	22	11	37
	C_{10}-AzoCOF	16	35	8.9	11	11	15	8.5	12
	H-AzoCOF	9.5	123	6.2	20	6.2	21	6.4	23
295 K	**Tg-AzoCOF**	22	23	6.9	7.6	7.2	7.9	7.7	8.7
	C_{10}-AzoCOF	14	22	6.6	6.9	8.3	9.0	6.5	6.9
	H-AzoCOF	12	17	7.0	6.3	7.4	5.7	6.3	5.2

[a]Total pressure: 1 bar; molar ratio: 50:50. [b]The selectivity obtained from the second run.

Table 3. Gas Selectivity of AzoCOFs Series in Comparison to the Selected Other Porous Materials

porous materials	C_2H_2/CH_4	C_2H_4/CH_4	C_2H_6/CH_4	CO_2/CH_4	reference
Tg-AzoCOF	2891	18	22	37	this work
C_{10}-AzoCOF	35	11	15	12	this work
H-AzoCOF	123	20	21	23	this work
Cu-TDPAT	154.3	124.7	16.4		22
Hexene-CTF_500_10	24.5	14.8		9.6	13
UTSA_38a	6.5	4.9	5.7	3.6	23
UTSA_36a	16.1	14.7	24.7		24
HOF-BTB	12.5	10.9	17.7		25
$[Mn(INA)_2]\cdot$ MeOH	515	64	71		26

selectivity of C_2H_4, C_2H_6, and CO_2 over CH_4 are comparable with other materials.

The gas adsorption selectivity of AzoCOFs largely drops at 295 K. At the elevated temperature, **Tg-AzoCOF** still shows a higher selectivity toward unsaturated C2 and CO_2 over methane when compared to **C_{10}-AzoCOF** and **H-AzoCOF**. However, the difference in gas adsorption selectivity of the three COFs is significantly reduced at 295 K. The IAST selectivity of C_2H_2/CH_4 drops from 2891, 35, and 123 to 23, 22, and 17, respectively, for **Tg-AzoCOF**, **C_{10}-AzoCOF**, and **H-AzoCOF** when the temperature is raised from 273 to 295 K. At a low temperature, enthalpy is the key factor, whereas entropy is a more important factor at a high temperature. Thus, when enthalpy dominates at a low temperature, **Tg-AzoCOF** with high affinities toward acetylene and CO_2 shows dramatically higher C_2H_2/CH_4 and CO_2/CH_4 selectivity than **C_{10}-AzoCOF** and **H-AzoCOF**. When entropy becomes the key factor at a higher temperature, the molecular interactions between absorbates and absorbents play a less important role, causing the difference between gas adsorption selectivity of AzoCOFs less pronounced.

Next, we estimated the isosteric heats (Q_{st}) of CH_4, C_2H_2, C_2H_4, C_2H_6, and CO_2 adsorption to further understand the gas adsorption affinities and the selective adsorption properties. Q_{st} were calculated from the adsorption isotherms at 273 and 295 K by using virial-type expressions; the Q_{st}.

For all AzoCOFs at zero coverage, Q_{st} are summarized in Table 4. For methane, **C_{10}-AzoCOF** has the highest isosteric heat (22.86 kJ/mol) and **H-AzoCOF** has the lowest (9.98 kJ/mol). For acetylene, **Tg-AzoCOF** has the highest isosteric heat (34.01 kJ/mol), which supports its remarkably high acetylene adsorption selectivity. **H-AzoCOF** has the highest isosteric heats for C_2H_4 (30.61 kJ/mol), C_2H_6 (33.29 kJ/mol), and CO_2 (38.22 kJ/mol), due to its highest surface area.

Table 4. Summary of Q_{st} of AzoCOF Series at Zero coverage[a]

samples	CH_4	C_2H_2	C_2H_4	C_2H_6	CO_2
Tg-AzoCOF	14.85	34.01	27.40	31.43	36.11
C_{10}-AzoCOF	22.86	32.64	28.07	22.71	34.59
H-AzoCOF	9.98	33.10	30.61	33.29	38.22

[a]Unit of Q_{st}: kJ/mol.

To further prove the critical role of azo groups, we also synthesized the known **H-COF** without azo substituents as a control COF.[20,21] The PXRD patterns of **H-COF** match well with the literature reports.[21] The IAST calculation shows that the selectivity of C_2H_2/CH_4 of **H-COF** is around 35 at 273 K, far lower than that of **H-AzoCOF** (123), which has a comparable high surface area but no extra alkyl or Tg chains (Figures S57–S59). **H-COF** also shows a much lower Q_{st} of C_2H_2 adsorption (29.51 kJ/mol) compared to all three AzoCOFs (Figures S60–S63). These results further support the critical role of azo groups for selective C_2H_2 sorption. Although azobenzene moieties can undergo *trans*/*cis* photoisomerization, we did not observe any significant change (only a 2.7% increase in the uptake) in the CO_2 adsorption capacity of **H-AzoCOF** after irradiating the sample with a mercury lamp for 10 min, indicating that the conformational change of the bulky azobenzene substituents, attached to the backbone of the COF and immobilized in the pores, is likely very limited.

4. CONCLUSION

In summary, we have successfully synthesized a series of AzoCOFs with azo groups incorporated as the side chains through imine condensation. This represents the first example of imine-linked crystalline COFs with azo groups pointing

inside the pores as the substituents, which are applied toward C2/C1 separation application. All the AzoCOFs show excellent to good IAST selectivity for C_2H_2 (up to 2891), C_2H_4 (up to 20), C_2H_6 (up to 22), and CO_2 (up to 37) over methane at 273 K and 1 bar. The C_2H_2/CH_4 selectivity is the highest reported so far, while other gas pair selectivity is comparable with most of the porous materials. Our study shows that the gas adsorption selectivity strongly depends on both the surface area and polar environment inside the pores. By examining three framework structures with the same backbone but different substituents inside the pores, we revealed that a small surface area, azo groups, and high polarity chains all contribute to the observed gas adsorption selectivity. Our study provides an interesting aspect of azo groups, which potentially could play an important role in gas separation applications. For practical applications, simple COFs with azo groups that can be more easily scaled-up, cost effective, and regenerable are desired.

■ ASSOCIATED CONTENT

Supporting Information

The Supporting Information is available free of charge at https://pubs.acs.org/doi/10.1021/acsami.0c15328.

Materials and general methods, experimental procedures, solid-state 13C CP-MAS spectra of AzoCOFs, FTIR of AzoCOFs, powder X-ray diffraction of AzoCOFs, TGA of AzoCOFs, additional adsorption data of AzoCOFs, additional IAST calculation results of AzoCOFs, estimation of adsorption heat of AzoCOFs, gas adsorption properties of H-COF, estimation of adsorption heat of H-COF, TEM image of AzoCOF, NMR spectra of new compounds (PDF)

■ AUTHOR INFORMATION

Corresponding Authors

Shun Wan − *NCO Technologies, Longmont, Colorado 80501, United States;* orcid.org/0000-0002-4224-3719; Email: wan@ncotechs.com

Yinghua Jin − *NCO Technologies, Longmont, Colorado 80501, United States*; Email: jinalice@yahoo.com

Wei Zhang − *Department of Chemistry, University of Colorado, Boulder, Colorado 80309, United States;* orcid.org/0000-0002-5491-1155; Email: wei.zhang@colorado.edu

Authors

Shaofeng Huang − *Department of Chemistry, University of Colorado, Boulder, Colorado 80309, United States;* orcid.org/0000-0002-2565-0005

Yiming Hu − *Department of Chemistry, University of Colorado, Boulder, Colorado 80309, United States*

Li-Li Tan − *State Key Laboratory of Solidification Processing, Center for Nano Energy Materials, School of Materials Science and Engineering, Northwestern Polytechnical University and Shaanxi Joint Laboratory of Graphene (NPU), Xi'an 710072, China*

Sadegh Yazdi − *Renewable and Sustainable Energy Institute, University of Colorado Boulder, Boulder, Colorado 80309, United States;* orcid.org/0000-0002-3470-9398

Complete contact information is available at: https://pubs.acs.org/10.1021/acsami.0c15328

Notes

The authors declare no competing financial interest.

■ ACKNOWLEDGMENTS

We thank Prof. D. Gin (University of Colorado Boulder) for the PXRD and TGA facilities support, the Department of Energy (DE-SC0017246), the University of Colorado Boulder, and the K.C. Wong Education Foundation for the financial support.

■ REFERENCES

(1) Colten, O. A. Basic Raw Materials in the Petrochemical Industry. *Industrial & Engineering Chemistry* **1959**, *51*, 983−984.

(2) Côté, A. P.; Benin, A. I.; Ockwig, N. W.; O'Keeffe, M.; Matzger, A. J.; Yaghi, O. M. Porous, Crystalline, Covalent Organic Frameworks. *Science* **2005**, *310*, 1166−1170.

(3) Furukawa, H.; Yaghi, O. M. Storage of Hydrogen, Methane, and Carbon Dioxide in Highly Porous Covalent Organic Frameworks for Clean Energy Applications. *J. Am. Chem. Soc.* **2009**, *131*, 8875−8883.

(4) Doonan, C. J.; Tranchemontagne, D. J.; Glover, T. G.; Hunt, J. R.; Yaghi, O. M. Exceptional Ammonia Uptake by a Covalent Organic Framework. *Nat. Chem.* **2010**, *2*, 235−238.

(5) Han, S. S.; Furukawa, H.; Yaghi, O. M.; Goddard, W. A. Covalent Organic Frameworks as Exceptional Hydrogen Storage Materials. *J. Am. Chem. Soc.* **2008**, *130*, 11580−11581.

(6) Feng, X.; Ding, X.; Jiang, D. Covalent Organic Frameworks. *Chem. Soc. Rev.* **2012**, *41*, 6010−6022.

(7) Jin, Y.; Yu, C.; Denman, R. J.; Zhang, W. Recent Advances in Dynamic Covalent Chemistry. *Chem. Soc. Rev.* **2013**, *42*, 6634−6654.

(8) Jin, Y.; Hu, Y.; Zhang, W. Tessellated Multiporous Two-Dimensional Covalent Organic Frameworks. *Nat. Rev. Chem.* **2017**, *1*, 0056.

(9) Geng, K.; He, T.; Liu, R.; Dalapati, S.; Tan, K. T.; Li, Z.; Tao, S.; Gong, Y.; Jiang, Q.; Jiang, D. Covalent Organic Frameworks: Design, Synthesis, and Functions. *Chem. Rev.* **2020**, *120*, 8814−8933.

(10) Colson, J. W.; Dichtel, W. R. Rationally Synthesized Two-Dimensional Polymers. *Nat. Chem.* **2013**, *5*, 453−465.

(11) Ding, S.-Y.; Wang, W. Covalent Organic Frameworks (COFs): from Design to Applications. *Chem. Soc. Rev.* **2013**, *42*, 548−568.

(12) Ma, H.; Ren, H.; Meng, S.; Yan, Z.; Zhao, H.; Sun, F.; Zhu, G. A 3D Microporous Covalent Organic Framework with Exceedingly High C3H8/CH4 and C2 Hydrocarbon/CH4 Selectivity. *Chem. Commun.* **2013**, *49*, 9773−9775.

(13) Krishnaraj, C.; Jena, H. S.; Leus, K.; Freeman, H. M.; Benning, L. G.; Van Der Voort, P. An Aliphatic Hexene-Covalent Triazine Framework for Selective Acetylene/Methane and Ethylene/Methane Separation. *J. Mater. Chem. A* **2019**, *7*, 13188−13196.

(14) Patel, H. A.; Hyun Je, S.; Park, J.; Chen, D. P.; Jung, Y.; Yavuz, C. T.; Coskun, A. Unprecedented High-Temperature CO2 Selectivity in N2-Phobic Nanoporous Covalent Organic Polymers. *Nat. Commun.* **2013**, *4*, 1357.

(15) Arab, P.; Rabbani, M. G.; Sekizkardes, A. K.; İslamoğlu, T.; El-Kaderi, H. M. Copper(I)-Catalyzed Synthesis of Nanoporous Azo-Linked Polymers: Impact of Textural Properties on Gas Storage and Selective Carbon Dioxide Capture. *Chem. Mater.* **2014**, *26*, 1385−1392.

(16) Lu, J.; Zhang, J. Facile Synthesis of Azo-Linked Porous Organic Frameworks via Reductive Homocoupling for Selective CO2 Capture. *J. Mater. Chem. A* **2014**, *2*, 13831−13834.

(17) Yang, Z.; Zhang, H.; Yu, B.; Zhao, Y.; Ma, Z.; Ji, G.; Han, B.; Liu, Z. Azo-Functionalized Microporous Organic Polymers: Synthesis and Applications in CO2 Capture and Conversion. *Chem. Commun.* **2015**, *51*, 11576−11579.

(18) Myers, A. L.; Prausnitz, J. M. Thermodynamics of Mixed-Gas Adsorption. *AIChE J.* **1965**, *11*, 121−127.

(19) We repeated the experiment with two different batches of Tg-AzoCOF samples (150 mg and 180 mg of the materials used) to confirm such high IAST selectivity. We elongated the equilibrium

time to 5 min to ensure accurate masurement of the gas uptake at low pressure range. The C_2H_2/CH_4 IAST selectivities of Tg-AzoCOF in the two independent runs were 2891 and 2426.

(20) Pachfule, P.; Acharjya, A.; Roeser, J.; Langenhahn, T.; Schwarze, M.; Schomäcker, R.; Thomas, A.; Schmidt, J. Diacetylene Functionalized Covalent Organic Framework (COF) for Photocatalytic Hydrogen Generation. *J. Am. Chem. Soc.* **2018**, *140*, 1423−1427.

(21) Karak, S.; Kandambeth, S.; Biswal, B. P.; Sasmal, H. S.; Kumar, S.; Pachfule, P.; Banerjee, R. Constructing Ultraporous Covalent Organic Frameworks in Seconds via an Organic Terracotta Process. *J. Am. Chem. Soc.* **2017**, *139*, 1856−1862.

(22) Liu, K.; Ma, D.; Li, B.; Li, Y.; Yao, K.; Zhang, Z.; Han, Y.; Shi, Z. High Storage Capacity and Separation Selectivity for C2 Hydrocarbons over Methane in the Metal−Organic Framework Cu−TDPAT. *J. Mater. Chem. A* **2014**, *2*, 15823−15828.

(23) Das, M. C.; Xu, H.; Wang, Z.; Srinivas, G.; Zhou, W.; Yue, Y.-F.; Nesterov, V. N.; Qian, G.; Chen, B. A Zn4O-Containing Doubly Interpenetrated Porous Metal−Organic Framework for Photocatalytic Decomposition of Methyl Orange. *Chem. Commun.* **2011**, *47*, 11715−11717.

(24) Das, M. C.; Xu, H.; Xiang, S.; Zhang, Z.; Arman, H. D.; Qian, G.; Chen, B. A New Approach to Construct a Doubly Interpenetrated Microporous Metal−Organic Framework of Primitive Cubic Net for Highly Selective Sorption of Small Hydrocarbon Molecules. *Chem. − Eur. J.* **2011**, *17*, 7817−7822.

(25) Yoon, T.-U.; Baek, S. B.; Kim, D.; Kim, E.-J.; Lee, W.-G.; Singh, B. K.; Lah, M. S.; Bae, Y.-S.; Kim, K. S. Efficient Separation of C2 Hydrocarbons in a Permanently Porous Hydrogen-Bonded Organic Framework. *Chem. Commun.* **2018**, *54*, 9360−9363.

(26) Lin, R.-G.; Li, L.; Lin, R.-B.; Arman, H.; Chen, B. Separation of C2/C1 Hydrocarbons through a Gate-Opening Effect in a Microporous Metal−Organic Framework. *CrystEngComm* **2017**, *19*, 6896−6901.